Bound-State Formation of Quantum Many-Flavor Systems: The Divergence of the Critical Coupling

Tyler Blanton
Advisor: Joaquín Drut

April 27, 2016

Abstract

When multiple quantum particles of different species – or "flavors" – are allowed to interact via pairwise interactions, they may form bound states. If these interactions can be modeled by an attractive contact potential, the strength of the attractions will depend on a single parameter: the coupling g. In 3D, when two or more flavors are present, it is possible for the system to form a bound state if the coupling is above a certain finite threshold g_c. In contrast, a one-flavor system is just a free particle and can only exist in scattering states (i.e., $g_c = \infty$). Although non-integer flavor numbers N_f have no obvious physical meaning, they are mathematically valid and can be used to examine the analytic relationship between N_f and g_c. We used computational methods to vary N_f in the continuum interval $(1, 2]$ in an effort to determine the manner in which $g_c \to \infty$ as $N_f \to 1^+$. We used Fortran and Python to calculate many-body quantum systems with parameters N_f and g. Specifically, we used the projection Monte Carlo method to calculate the ground-state energies E_0 of these systems. Plotting E_0 vs. g, we obtained the critical coupling g_c at which bound state formation occurred for each N_f sampled. Determining the manner in which g_c diverges sees applications in theoretical fields such as QCD – where similar problems related to flavor number arise in the study of quarks – as well as in the experimental study of ultracold atoms, where the quantum simulation of increasingly arbitrary systems is becoming a reality.

Chapter 1

Introduction

In 1970, V. N. Efimov mathematically showed that when three particles interact via a pairwise potential tuned to unitarity (the scale-invariant threshold for two-body bound-state formation), they should display an infinite sequence of three-body bound states [1, 2]. The experimental confirmation of Efimov's predictions did not come until much more recently, as detailed in Refs. [3, 4]. With the continued improvement of experimental techniques used to study ultra-cold atoms, the quantum simulation of arbitrary systems have become increasingly possible. Perhaps the most successful technique developed so far is the utilization of Feshbach resonance, where a system's interaction is tuned to unitarity – at which point bond lengths become infinite – by varying the frequency of a magnetic field [5].

There are several different scales that can exist in a many-body system. For the sake of simplicity we only discuss three: one associated with the interaction range r_0, one with the inter-particle spacing d_0, and one with the temperature T. The associated energy scales (in units where $\hbar = m = k_B = 1$) are r_0^{-2}, d_0^{-2}, and T. The relationship between d_0^{-2}, which is a measure of the particle density, and the temperature scale T determine whether or not the system is truly quantum mechanical. For example, when $T \ll d_0^{-2}$, phenomena such as Bose-Einstein condensation (BEC) and the formation of Cooper pairs become possible. In this paper, we are interested in the near-unitary case where the interaction scale r_0^{-2} is extremely large compared to d_0^{-2} and T; i.e., where the system is very dilute in relation to the scale of the interaction energies.

Chapter 2

Theory

2.1 General Many-Body Formalism

For a many-fermion quantum system subject to a pairwise attractive contact potential, the Hamiltonian takes the form

$$\hat{H} = \hat{T} + \hat{V}, \tag{2.1}$$

where

$$\hat{T} \equiv \sum_{s=1}^{N_f} \int d^3p \ \frac{p^2}{2m} \ \hat{a}^\dagger_{\mathbf{p},s} \hat{a}_{\mathbf{p},s} \ , \tag{2.2}$$

$$\hat{V} \equiv \frac{1}{2} \sum_{s \neq s'}^{N_f} \hat{V}_{s,s'}, \tag{2.3}$$

and

$$\hat{V}_{s,s'} = -g \int d^3x \ \hat{n}_s(\mathbf{x}) \hat{n}_{s'}(\mathbf{x}). \tag{2.4}$$

In these equations, N_f is the number of different particle flavors, $\hat{a}^{(\dagger)}_{\mathbf{p},s}$ is the annihilation (creation) operator for particles of flavor s and momentum $\mathbf{p}$, and $\hat{n}_s(\mathbf{x})$ is the coordinate-space density operator for particles of flavor s at position $\mathbf{x}$, and g is the bare coupling of the pairwise interaction potential. For this paper, we assume that the species are uniformly distributed with N particles of each flavor so that the total number of fermions in the system is $N_{tot} = N_f N$.

Our goal is to extract the ground-state energy E_0 of this system. We do so by applying the projection operator $\exp(-\beta\hat{H})$ to a guess state $|\Psi\rangle$, which is not orthogonal to the true ground state, and taking the limit $\beta \to \infty$ (see Ref. [6] for detailed accounts of various methods). Defining $N_\tau \in \mathbb{N}$ and the corresponding $\tau \in \mathbb{R}^+$ such that $\tau N_\tau \equiv \beta$, we rewrite the projection operator as a product of imaginary time transfer matrices:

$$e^{-\beta\hat{H}} = \prod_{j=1}^{N_\tau} e^{-\tau_j \hat{H}}, \tag{2.5}$$

where $\tau_j \equiv \tau$ for each j; the index is just to keep track of the time step. At each step j, we separate the kinetic and potential energy terms using a symmetric Suzuki-Trotter decomposition:

$$e^{-\tau_j \hat{H}} = e^{-\tau_j \hat{T}/2} e^{-\tau_j \hat{V}} e^{-\tau_j \hat{T}/2} + O(\tau^3). \tag{2.6}$$

Since the kinetic energy matrix is diagonal in momentum space, it is easy to work with via Fourier Transforms. The potential energy term is a bit trickier due to the coupled density operators in each two-body interaction term:

$$\begin{aligned} e^{-\tau_j \hat{V}} &= \exp\left[\frac{\tau_j g}{2} \sum_{s \neq s'} \int d^3x \; \hat{n}_s(\mathbf{x}) \hat{n}_{s'}(\mathbf{x})\right] \\ &= \prod_{s \neq s'} \prod_{\mathbf{x}} e^{\frac{\tau_j g}{2} \hat{n}_s(\mathbf{x}) \hat{n}_{s'}(\mathbf{x})}, \end{aligned}$$

where the second product is continuous over all space (though in practice it is normally approximated as a discrete product).

We next decouple the density operators on the RHS of Eq. (2.7) using a Hubbard-Stratonovich transformation (Refs. [7, 8]) to introduce a field integral:

$$e^{\frac{\tau_j g}{2} \hat{n}_s(\mathbf{x}) \hat{n}_{s'}(\mathbf{x})} = \int_{-\pi}^{\pi} \frac{d\sigma[\mathbf{x}, \tau_j, s, s']}{2\pi} \left[1 + (A\sqrt{2}\sin\sigma)\hat{n}_s(\mathbf{x})\right] \left[1 + (A\sqrt{2}\sin\sigma)\hat{n}_{s'}(\mathbf{x})\right], \tag{2.7}$$

where $A = \sqrt{e^{\tau g/2} - 1}$ and $\sigma[\mathbf{x}, \tau_j, s, s']$ is an auxiliary field, where the arguments are really just indices to serve as a reminder that there is a different integral for every point in space, each time slice j, and every flavor pair (s, s'). For convenience we also define

$$e^{-\hat{V}_{s(s')}[\sigma]} \equiv 1 + (A\sqrt{2}\sin\sigma)\hat{n}_{s(s')}(\mathbf{x}). \tag{2.8}$$

Plugging everything into Eq. (2.5) and rearranging, we have:

$$e^{-\beta \hat{H}} = \prod_{j=1}^{N_\tau} \left[e^{-\frac{\tau_j \hat{T}}{2}} \prod_{s \neq s'}^{N_f} \prod_{\mathbf{x}} \left(\int_{-\pi}^{\pi} \frac{d\sigma[\mathbf{x}, \tau_j, s, s']}{2\pi} e^{-\hat{V}_s[\sigma]} e^{-\hat{V}_{s'}[\sigma]} \right) e^{-\frac{\tau_j \hat{T}}{2}} \right] \tag{2.9}$$

$$= \left(\prod_{j=1}^{N_\tau} \prod_{s \neq s'}^{N_f} \prod_{\mathbf{x}} \int_{-\pi}^{\pi} \frac{d\sigma}{2\pi} \right) \left[\prod_{j=1}^{N_\tau} e^{-\frac{\tau_j \hat{T}}{2}} \left(\prod_{s \neq s'}^{N_f} \prod_{\mathbf{x}} e^{-\hat{V}_s[\sigma]} e^{-\hat{V}_{s'}[\sigma]} \right) e^{-\frac{\tau_j \hat{T}}{2}} \right] \tag{2.10}$$

$$= \int \mathcal{D}\sigma[\mathbf{x}, \tau_j, s, s'] \prod_{j=1}^{N_\tau} B_j[\sigma], \tag{2.11}$$

where

$$\hat{B}_j[\sigma] \equiv e^{-\frac{\tau_j \hat{T}}{2}} \left(\prod_{s \neq s'}^{N_f} \prod_{\mathbf{x}} e^{-\hat{V}_s[\sigma]} e^{-\hat{V}_{s'}[\sigma]} \right) e^{-\frac{\tau_j \hat{T}}{2}}, \tag{2.12}$$

and the path integral is over all space, time slices, and flavor pairs.

We then define the "partition sum" $\mathcal{Z}$ as an approximation of the canonical partition function:

$$\mathcal{Z} \equiv \langle\Psi|\, e^{-\beta\hat{H}}\, |\Psi\rangle = \int \mathcal{D}\sigma[\mathbf{x}, \tau_j, s, s']\, \langle\Psi| \prod_{j=1}^{N_\tau} \hat{B}_j[\sigma]\, |\Psi\rangle\,, \tag{2.13}$$

where $|\Psi\rangle$ is our trial ket for the ground state of the system with wavefunction

$$\Psi(\mathbf{x}_1, \mathbf{x}_2, \ldots, \mathbf{x}_{N_{tot}}) \equiv \langle \mathbf{x}_1, \mathbf{x}_2, \ldots, \mathbf{x}_{N_{tot}} | \Psi\rangle = \prod_{i=1}^{N_f} \psi_{s_i}(\mathbf{x}_1, \mathbf{x}_2, \ldots, \mathbf{x}_N), \tag{2.14}$$

and each ψ_{s_i} is a Slater determinant

$$\psi_{s_i}(\mathbf{x}_1, \mathbf{x}_2, \ldots, \mathbf{x}_N) = \frac{1}{\sqrt{N!}} \begin{vmatrix} \chi_1^{s_i}(\mathbf{x}_1) & \chi_2^{s_i}(\mathbf{x}_1) & \cdots & \chi_N^{s_i}(\mathbf{x}_1) \\ \chi_1^{s_i}(\mathbf{x}_2) & \chi_2^{s_i}(\mathbf{x}_2) & \cdots & \chi_N^{s_i}(\mathbf{x}_2) \\ \vdots & \vdots & \ddots & \vdots \\ \chi_1^{s_i}(\mathbf{x}_N) & \chi_2^{s_i}(\mathbf{x}_N) & \cdots & \chi_N^{s_i}(\mathbf{x}_N) \end{vmatrix} \tag{2.15}$$

of the single-particle spin-orbital wavefunctions $\chi_k^{s_i}(\mathbf{x}_l)$ for the N fermions of flavor s_i. While this initial guess can certainly be optimized, it is sufficient for our purposes in the $\beta \to \infty$ limit.

Define $|\Psi\rangle$ as the ket corresponding to Ψ. Returning to Eq. (2.13), we have:

$$\mathcal{Z} = \int \mathcal{D}\sigma[\mathbf{x}, \tau_j, s, s']\, \langle\Psi| \prod_{j=1}^{N_\tau} B_j[\sigma]\, |\Psi\rangle = \int \mathcal{D}\sigma[\mathbf{x}, \tau_j, s, s'] (\det \mathcal{U}[\sigma])^{N_f}, \tag{2.16}$$

where

$$[\mathcal{U}]_{i,j} = \langle i|\, \hat{B}_{N_\tau} \hat{B}_{N_\tau - 1} \cdots \hat{B}_2 \hat{B}_1\, |j\rangle\,, \tag{2.17}$$

and $\{|i\rangle\}_{i=1}^{N}$ are the single-particle states in the Slater determinant for a given species of fermions. If $(\det \mathcal{U})^{N_f}$ is positive semi-definite for all auxiliary field configurations, it is natural to define the probability of obtaining a certain configuration $\sigma[\mathbf{x}, \tau_j, s, s']$ as

$$P[\sigma] \equiv \frac{1}{\mathcal{Z}} (\det \mathcal{U}[\sigma])^{N_f}. \tag{2.18}$$

The average total energy of the system $\langle E\rangle_\beta$ can then be expressed as

$$\langle E\rangle_\beta = -\frac{\partial \ln \mathcal{Z}}{\partial \beta} = -\frac{1}{\mathcal{Z}} \int \mathcal{D}\sigma \frac{\partial}{\partial \beta} (\det \mathcal{U}[\sigma])^{N_f} \tag{2.19}$$

$$= \int \mathcal{D}\sigma \left[\frac{(\det \mathcal{U})^{N_f}}{\mathcal{Z}}\right] \left[-N_f \operatorname{Tr}\left(\mathcal{U}^{-1} \frac{\partial \mathcal{U}}{\partial \beta}\right)\right] \tag{2.20}$$

$$\equiv \int \mathcal{D}\sigma\ P[\sigma] E[\sigma], \tag{2.21}$$

where Eq. (2.20) follows from the identity $\det\mathcal{U} = \exp[\mathrm{Tr}(\ln\mathcal{U})]$, and Eq. (2.21) follows directly from the definition of $\langle E\rangle$ with $E[\sigma]$ representing the energy of the particular field configuration σ. Using Eq. (2.18) as the definition of $P[\sigma]$, it is natural to then define

$$E[\sigma] \equiv -N_f \,\mathrm{Tr}\left(\mathcal{U}^{-1}\frac{\partial\mathcal{U}}{\partial\beta}\right) \tag{2.22}$$

to satisfy Eq. (2.20) and thus make our formalism self-consistent.

Lastly, it can be shown that in the $\beta\to\infty$ limit, $\langle E\rangle_\beta$ is related to the ground-state energy E_0 as

$$\langle E\rangle_\beta \overset{\beta\to\infty}{\longrightarrow} E_0 + e^{-\beta(E_1-E_0)}\frac{|c_1|^2}{|c_0|^2}(E_1-E_0), \tag{2.23}$$

where $c_n \equiv \langle E_n|\Psi\rangle$ is the projection of our trial state onto the nth energy eigenstate (see, e.g., Refs. [9, 10]). Thus as long as our guess $|\Psi\rangle$ is not orthogonal to the true ground state, we are guaranteed to have $\langle E\rangle_\beta$ decay exponentially to E_0 for large enough β. This rapid monotonic decay to the ground-state energy is crucial: it means that finite β can be used to calculate E_0.

The general theoretical approach can be summarized as follows:

1. Write down the Hamiltonian and the projection operator $e^{-\beta\hat{H}}$.
2. Decouple the kinetic and potential energy terms via a Suzuki-Trotter decomposition.
3. Decouple each two-body interaction potential into an integral of two single-body terms via a Hubbard-Stratonovich transformation.
4. Rewrite the projection operator as a path integral.
5. Define a trial state $|\Psi\rangle$ whose wavefunction is a product of Slater determinants.
6. Use $|\Psi\rangle$ to approximate the canonical partition function with the "partition sum" $\mathcal{Z}$.
7. Write out $-\frac{\partial\ln\mathcal{Z}}{\partial\beta}$ to get an expression for the average total energy $\langle E\rangle_\beta$.
8. Compute $\langle E\rangle_\beta$ in the $\beta\to\infty$ limit to obtain the ground-state energy E_0.

2.1.1 The Distinguishable Particles Case

In general, N_f is required to be an even integer in order to ensure that $P[\sigma] \propto (\det\mathcal{U}[\sigma])^{N_f}$ is positive semi-definite. However, in this paper we only consider the special case where all fermions are distinguishable (i.e., $N = 1$, $N_{tot} = N_f$). In this case, the determinant is unnecessary since the Slater determinant for each flavor is just the single-particle spin-orbital wavefunction $\chi_1^{s_i}(\mathbf{x}_1)$. Thus

$$\mathcal{U}[\sigma] = \langle 1|\,\hat{B}_{N_\tau}\hat{B}_{N_\tau-1}\cdots\hat{B}_2\hat{B}_1\,|1\rangle \tag{2.24}$$

is just a positive real number, where the sign can be obtained by noticing that each term in the equation for $\hat{B}_i[\sigma]$ (Eq. (2.12)) is positive. Therefore Eqs. (2.18) and (2.22) are reduced to

$$P[\sigma] = \frac{1}{\mathcal{Z}}(\mathcal{U}[\sigma])^{N_f} \tag{2.25}$$

$$E[\sigma] = -\frac{N_f}{\mathcal{U}[\sigma]}\frac{\partial \mathcal{U}[\sigma]}{\partial \beta}. \tag{2.26}$$

Notice that $P[\sigma]$ is now semi-positive definite for all real values of N_f, allowing us to choose any values we like – namely, values in the continuum interval $(1, 2]$.

2.2 Bound-State Formation

Consider taking the pairwise interaction potential $\hat{V}_{s,s'}$ defined in Eq. (2.4) for a system of $N_f \geq 2$ distinguishable particles and slowly increasing the bare coupling g from zero. At $g = 0$, the potential term vanishes and the particles move as free particles in scattering states ($E > 0$). As g is slowly increased, the attractions between the particles becomes stronger and a potential well begins to form. In 3D, the solution to the two-body Schrödinger equation reveals that systems of this type are guaranteed to form a bound state once g reaches a certain threshold g_c called the critical coupling. The more particles there are, the more effectively attractive the potential for a given coupling. As a result, systems with large numbers of particles are able to form bound states for weaker couplings than those required for bound-state formation in few-particle systems; i.e., g_c decreases with N_f.

An interesting consequence of this inverse relationship is that an N_f-body system with a coupling g just above its critical coupling $g_c(N_f)$ will be in a bound state, but removing any one of the particles will cause the resulting $(N_f - 1)$-body system to be in a scattering state since $g \approx g_c(N_f) < g_c(N_f - 1)$. This type of N_f-body state is called a Borromean state in reference to the Borromean rings, which are all connected but would completely separate if any one ring was removed (see Fig. 2.1).

An analytic form for $g_c(N_f)$ is as of yet unknown. All that is known is that the critical coupling decreases monotonically for $N_f \geq 2$, and that in the trivial case $N_f = 1$ (i.e., a single free particle), it is obvious that a bound state cannot form for any coupling, so it is natural to set $g_c(1) = \infty$. Thus a possible prediction for an analytic form of the critical coupling might be

$$g_c(N_f) = a + \frac{b}{(N_f - 1)^c} \tag{2.27}$$

for some $a, b, c > 0$. To determine whether such a model is correct, one must first understand the manner in which the critical coupling diverges as $N_f \to 1^+$, which requires knowledge about values of $g_c(N_f)$ for N_f near unity; i.e., in the continuum interval $(1, 2]$. This was the goal of our project: to determine an analytic form that correctly models the divergence behavior of the critical coupling by computing $g_c(N_f)$ for $N_f \in (1, 2]$ and fitting the resulting data.

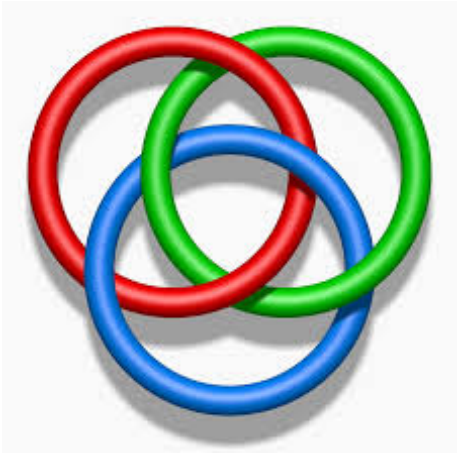

Figure 2.1: The Borromean rings (image from Wikipedia). Notice that all three are connected, but removing any one ring causes the other two to separate – very much analogous to bound-state formation of an N_f-body system just above its critical coupling $g_c(N_f)$.

Chapter 3

Methodology

3.1 Nondimensionalization and Scaling of Parameters

To model the system on a computer, we discretize (3+1)-dimensional Euclidean space-time into an $N_x^3 \times N_\tau$ lattice with boundary conditions that are periodic in the spatial directions and anti-periodic in the temporal direction. Since computers can only perform calculations with dimensionless quantities, we must first nondimensionalize all of the physical parameters we are interested in before inputting them for computation. We therefore use atomic units ($m = \hbar = 1$) so that all quantities can be made unitless. We then define the lattice spacing to be $\ell = 1$ in the spatial directions and τ in the temporal direction.

It is also advisable to define an energy scale ε for the system and work with $\langle E \rangle_\beta \, \varepsilon^{-1}$ and $\beta\varepsilon$, which are dimensionless in all unit systems and give a better sense of the magnitude of $\langle E \rangle_\beta$ and β relative to the scale of the system. In this spirit, we introduce the Fermi energy ε_F and free-gas energy E_{FG} of the system (in atomic units):

$$\varepsilon_F = \frac{\hbar^2}{2m}(6\pi^2)^{\frac{2}{3}} N_x^{-2} = \frac{1}{2}(6\pi^2)^{\frac{2}{3}} N_x^{-2} \tag{3.1}$$

$$E_{FG} = \frac{3}{5} N_f \varepsilon_F = \frac{3}{10}(6\pi^2)^{\frac{2}{3}} N_f N_x^{-2}. \tag{3.2}$$

Thus the scaled, nondimensionalized parameters that the computer will work with are:

$$\frac{\langle E \rangle_\beta}{E_{FG}} = \frac{10}{3}(6\pi^2)^{-\frac{2}{3}} N_x^2 \langle E \rangle_\beta \tag{3.3}$$

$$\beta\varepsilon_F = \frac{1}{2}(6\pi^2)^{\frac{2}{3}} N_x^{-2} \beta \propto \frac{\tau N_\tau}{N_x^2}. \tag{3.4}$$

Hence the lattice and the many-fermion system can be completely defined in the computer by the input parameters N_x, τ, N_f, g, and $\beta\varepsilon_F$.

To compute the nondimensionalized ground-state energy $E_0 E_{FG}^{-1}$ from these inputs, we take $\beta\varepsilon_F$ sufficiently large to ensure $\langle E \rangle_\beta \approx E_0$ (see Section 4.1) and have our program evaluate the path integral in Eq. (2.21) via a stochastic integration method: the Hybrid Monte Carlo (HMC) algorithm.

3.2 Hybrid Monte Carlo

Hybrid Monte Carlo (sometimes called Hamiltonian Monte Carlo) is a stochastic method developed in Ref. [11] and analyzed in detail in Ref. [12]. The idea is to create a set $\{\mathbf{q}_k \in \mathbb{R}^d\}_{k=1}^{N_s}$ that represents a random sampling of a probability distribution of the form

$$P(\mathbf{q}) \propto e^{-f(\mathbf{q})}, \tag{3.5}$$

by introducing a new random variable $\mathbf{p} \in \mathbb{R}^d$ that obeys a Gaussian probability distribution with variance M:

$$G(\mathbf{p}) \propto e^{-\mathbf{p}^T\mathbf{p}/2M}, \tag{3.6}$$

and working with the joint probability distribution

$$\tilde{P}(\mathbf{q},\mathbf{p}) = P(\mathbf{q})G(\mathbf{p}) \propto \exp\left[-\left(\frac{\mathbf{p}^T\mathbf{p}}{2M} + f(\mathbf{q})\right)\right] = e^{-H(\mathbf{q},\mathbf{p})}, \tag{3.7}$$

where $H(\mathbf{q},\mathbf{p}) \equiv \frac{\mathbf{p}^T\mathbf{p}}{2M} + f(\mathbf{q})$.

It is no accident that the choice of variable names coincides with the standard notation of Hamiltonian dynamics. After initial conditions $(\mathbf{q}_1, \mathbf{p}_1)$ are chosen (with $\mathbf{q}_1$ saved as the first member of the Markov chain), they are evolved in time according to Hamilton's equations:

$$\frac{\partial H}{\partial q_i} = -\dot{p}_i, \quad \frac{\partial H}{\partial p_i} = \dot{q}_i \tag{3.8}$$

for $i = 1, 2, \ldots, d$. After the coordinates evolve for a specified amount of time, the $\mathbf{p}$ coordinate is negated to make the process time-reversal symmetric. The resulting coordinates $(\mathbf{q}_1^*, \mathbf{p}_1^*)$ are then used to determine the next member of the Markov chain in a Metropolis update: $\mathbf{q}_1^*$ is accepted as the next member of the chain $(\mathbf{q}_2 = \mathbf{q}_1^*)$ with probability

$$\min\left(1, \frac{\tilde{P}(\mathbf{q}_1^*, \mathbf{p}_1^*)}{\tilde{P}(\mathbf{q}_1, \mathbf{p}_1)}\right) = \min\left(1, e^{H(\mathbf{q}_1,\mathbf{p}_1) - H(\mathbf{q}_1^*,\mathbf{p}_1^*)}\right). \tag{3.9}$$

If the new coordinates are rejected, the previous member of the Markov chain is repeated $(\mathbf{q}_2 = \mathbf{q}_1)$. After the chain is updated, $\mathbf{q}$ is left equal to $\mathbf{q}_2$, but a new $\mathbf{p}$ is randomly chosen from its Gaussian distribution $G(\mathbf{p})$. Since $\mathbf{q}$ and $\mathbf{p}$ are independent in $\tilde{P}(\mathbf{q},\mathbf{p})$, holding $\mathbf{q}$ constant while sampling a new $\mathbf{p}$ from its distribution G amounts to taking a new sample of coordinates from $\tilde{P}$. When these coordinates are evolved in time, the independence of $\mathbf{q}$ and $\mathbf{p}$ ensures that they both represent samples taken from their respective distributions P and G. This procedure is repeated until the Markov chain contains the desired number of samples N_s, at which point the resulting set $\{\mathbf{q}\}_{k=1}^{N_s}$ represents a random sampling of the probability distribution $P(\mathbf{q})$.

One way to picture the HMC algorithm is that initial coordinates determine an energy shell, and then Hamiltonian dynamics move the coordinates around the surface of the shell. By choosing a new $\mathbf{p}$ at the beginning of each step, new energy shells are reached each time

to ensure that the Markov chain is able to reach all regions of the sample-space. It is worth noting that a random seed is used to initialize the HMC procedure, which has the potential to ruin the random sampling process if samples are correlated to the seed. To avoid this issue, we evolve the initial coordinates for a relatively long time to ensure that the seed is "forgotten" and that the samples are decorrelated.

Note that since the Hamiltonian (energy) is conserved in Hamiltonian dynamics, we should always have $H(\mathbf{q}_k, \mathbf{p}_k) \approx H(\mathbf{q}_k^*, \mathbf{p}_k^*)$, with the only possible source of a discrepancy being the computational error from integrating Hamilton's equations (which is done via a leapfrog method to preserve time-reversal symmetry [12]). Thus in the HMC algorithm, the acceptance probability at each step should always be very close to unity, making the process of collecting samples $\mathbf{q}$ run much faster than those of naive Monte Carlo methods that perform random walks to obtain new samples.

3.3 Computing the Energy

Our program evaluates the path integral in Eq. (2.21) by implementing the HMC algorithm with the auxiliary field σ taking the role of $\mathbf{q}$ with $d = N_x^3 N_\tau$. The probability distribution of σ is given by Eq. (2.26), though it must be rewritten to take the form of Eq. (3.5):

$$P[\sigma] = \frac{1}{\mathcal{Z}} e^{N_f \ln \mathcal{U}[\sigma]}. \tag{3.10}$$

At each step k in the Markov chain, each $\hat{B}_j[\sigma_k^*]$ (which on our lattice is represented by an $N_x^3 \times N_x^3$ matrix) is computed via Eq. (2.12) and used to calculate $\mathcal{U}[\sigma_k^*]$, which is in turn used to compute $P[\sigma_k^*]$ for the Metropolis update.

Once the Markov chain is complete, the path integral is approximated as

$$\langle E \rangle_\beta = \int \mathcal{D}\sigma[\mathbf{x}, \tau_j, s, s'] P[\sigma] E[\sigma] = \frac{1}{N_s} \sum_{k=1}^{N_s} E[\sigma_k] + O\left(\frac{1}{\sqrt{N_s}}\right), \tag{3.11}$$

where each $E[\sigma_k]$ is calculated via Eq. (2.26), and the leading order error is due to the Central Limit Theorem.

3.4 Summary of Computer Program

The inputs of our program are:

- General system parameters:
  - d: spatial dimension; always taken to be 3 for this project
  - N_x: size of lattice in each spatial dimension
  - $\beta\varepsilon_F$: unitless quantity used to fix β (ε_F is the Fermi energy)

  - τ: lattice spacing in temporal direction
  - N_f: number of fermion flavors
  - N: number of particles per flavor; always taken to be 1 for this project
  - g: bare coupling of the contact potential

- Hybrid Monte Carlo parameters:
  - N_{seed}: random seed used to initialize the algorithm
  - τ_{HMC}: average evolution time of Hamilton's equations
  - $d\tau_{HMC}$: temporal lattice spacing in HMC (for integrating Hamilton's equations)
  - N_s: number of samples to put into the Markov chain

The output is a list $\left\{\frac{E[\sigma_k]}{E_{FG}}\right\}_{k=1}^{N_s}$ of the energies (in units of the free-gas energy E_{FG}) of field configurations in the HMC Markov chain. From this list, we compute the average energy $\langle E \rangle_\beta$ and its uncertainty σ_E.

Chapter 4

Results

4.1 Determining a Reasonable $\beta\varepsilon_F$

Although we are interested in the $\beta \to \infty$ limit, it is unwise to take $\beta = \tau N_\tau$ as large as possible since it scales linearly with the number of time steps N_τ (assuming the temporal lattice spacing τ is fixed) and therefore with the total number of operations performed. Instead, it is more practical to find a relatively small $\beta\varepsilon_F$ that is still sufficiently large to ensure $\langle E \rangle_\beta \approx E_0$ in all cases [9].

We calculated $\langle E \rangle_\beta / E_{FG}$ for various $\beta\varepsilon_F$ with $N_x = 16$, our smallest spatial lattice size used, in an attempt to determine what minimum value of $\beta\varepsilon_F$ is sufficient to ensure that we are always working in the $\beta \to \infty$ limit. For concreteness, we considered the specific case $N_f = 2.0$ and $g = 5.0$. Our results (Table 4.1) showed that even for the smallest $\beta\varepsilon_F$ our program could test ($\beta\varepsilon_F = 0.01$), the system's average energy was zero (within statistical uncertainty). When we tested larger $\beta\varepsilon_F$, we continued to obtain $\langle E \rangle_\beta = 0$. We therefore concluded that the exponential decay to the ground-state energy must have already begun to converge for some $\beta\varepsilon_F < 0.01$; in other words, we had effectively reached the $\beta \to \infty$ limit for $\beta\varepsilon_F$ as small as 0.01. Furthermore, since the limit of the average energy convergence was zero (as opposed to a significantly negative value), we concluded that the critical coupling $g_c(2.0)$ must be larger than the $g = 5.0$ coupling we tested.

For the remainder of our tests, we elected to use $\beta\varepsilon_F = 0.20$ to eliminate any doubt that we were operating in the $\beta \to \infty$ limit. Since $\beta = (\varepsilon_F)^{-1}\beta\varepsilon_F \propto N_x^2(\beta\varepsilon_F)$, using larger lattice sizes renders larger β values for the same $\beta\varepsilon_F = 0.2$ and only further ensures the validity of the approximation $\langle E \rangle_\beta \approx E_0$.

4.2 Critical Coupling Data

Once we determined that $\beta\varepsilon_F = 0.2$ was sufficient for our purposes, we began running jobs to compute the energy $\langle E \rangle_\beta \approx E_0$ in units of the free-gas energy E_{FG} for various flavor numbers $N_f \in (1, 2]$, couplings $g \in [5, 10]$, and lattice sizes $N_x \in \{16, 18, 20\}$. The purpose of testing different N_x was to ensure that the critical coupling $g_c(N_f)$ – the point where

Table 4.1: Average energy of system for various $\beta\varepsilon_F$, with $N_f = 2.0$ and $g = 5.0$. Note that all energy values are within statistical uncertainty of zero, indicating that they reflect the $\beta \to \infty$ limit and that the ground-state energy is $E_0 \approx 0$; i.e., that $g_c(2.0) > 5.0$.

$\beta\varepsilon_F$	$\langle E \rangle_\beta / E_{FG}$	σ_E
0.01	-0.38	0.41
0.02	0.06	0.33
0.03	-0.27	0.31
0.04	-0.15	0.29
0.05	-0.29	0.30
0.10	-0.19	0.25
0.15	0.07	0.21
0.20	-0.09	0.25
0.25	-0.10	0.21

the energy first became negative – remained independent of the lattice size; i.e., that we did not see any finite-volume effects.

As can be seen from our data in Fig. 4.1, the ground-state energy follows the expected qualitative behavior: it remains zero for small couplings (i.e., only scattering states exist), but once the coupling surpasses a certain threshold g_c, a bound state forms and the energy becomes negative. Also notice g_c is more or less the same for all three lattice sizes tested in each of the plots (which are separated by flavor number N_f). This consistency is strong evidence that our results are indeed representative of those expected in the infinite-volume limit.

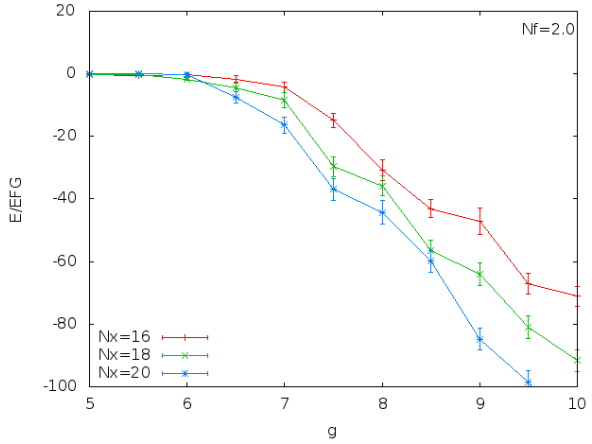

(a) $N_f = 2.0$, $g_c = 5.5 \pm 0.5$

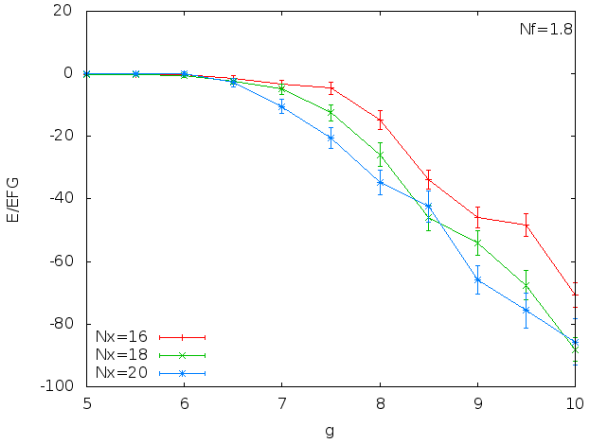

(b) $N_f = 1.8$, $g_c = 6.0 \pm 0.5$

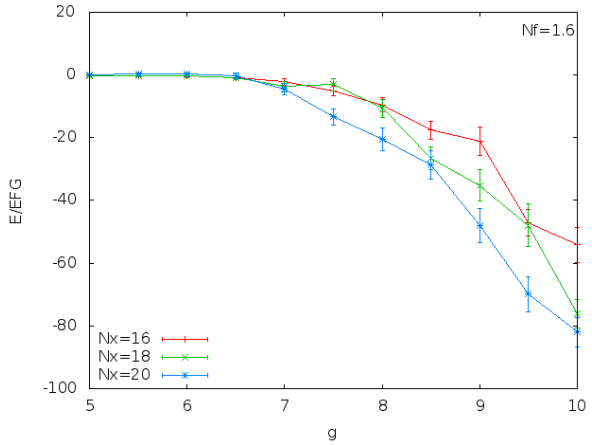

(c) $N_f = 1.6$, $g_c = 6.5 \pm 0.5$

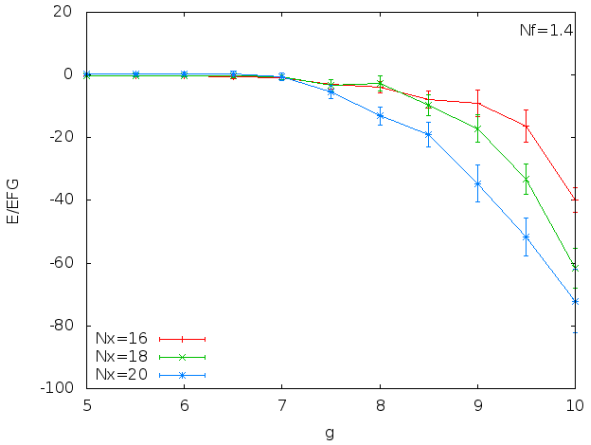

(d) $N_f = 1.4$, $g_c = 7.0 \pm 0.5$

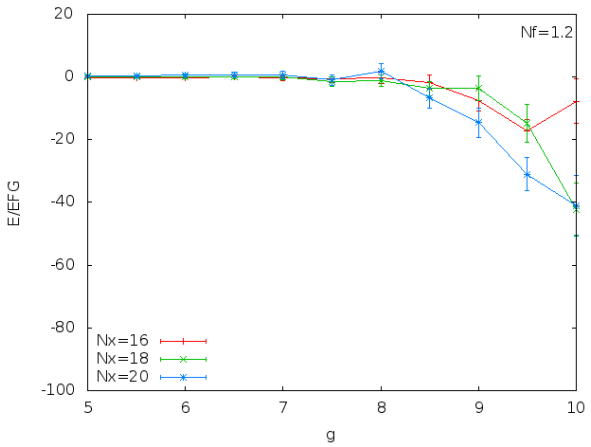

(e) $N_f = 1.2$, $g_c = 8.5 \pm 1.0$

Figure 4.1: Energy plotted against the coupling for various lattice sizes N_x and flavor numbers N_f. Notice that for each N_f, the critical coupling g_c where the energy begins to drop below zero is nearly the same for all three lattice sizes. Also note that a stronger coupling is required to form bound states for lower N_f as expected.

4.3 Fitting the Data

We lastly seek to find an analytic model for $g_c(N_f)$ that correctly fits all available data. To this end, we combine our $N_f \in (1, 2]$ data with $N_f > 2$ data collected by Philip Javernick (a graduate student of Dr. Joaquín Drut). We proceed assuming that $g_c(N_f)$ obeys the model proposed in Eq. (2.27). Taking the log of both sides yields a linear function in c:

$$\ln\left(g_c(N_f) - a\right) = -c\ln(N_f - 1) + \ln b, \tag{4.1}$$

which can be fit by optimizing b and c for fixed a using a least-squares regression. By varying a, optimizing the resulting b and c, and computing the resulting root-mean-square error E_{rms}, we define our optimized fitting parameters (a, b, c) as those which minimize E_{rms}.

Applying this procedure to the combination of $N_f \in (1, 2]$ and $N_f > 2$ data, we found the optimized fitting parameters to be $(a, b, c) = (1.66, 3.70, 0.50)$. The fitted function $g_c(N_f)$ with our optimized parameters (a, b, c) can be seen plotted over the actual data in Fig. 4.2. Our optimized guess for the analytic form of $g_c(N_f)$ is therefore:

$$g_c^{\text{fit}}(N_f) = 1.66 + \frac{3.70}{(N_f - 1)^{0.50}}. \tag{4.2}$$

This fit gives a root-mean-square error of $E_{rms} = 1.05$ when applied to the data, although most of the error is due to the $N_f = 1.2$ data point (which also has the largest error bars); if this point is removed from the analysis, the error drops to $E_{rms} = 0.25$.

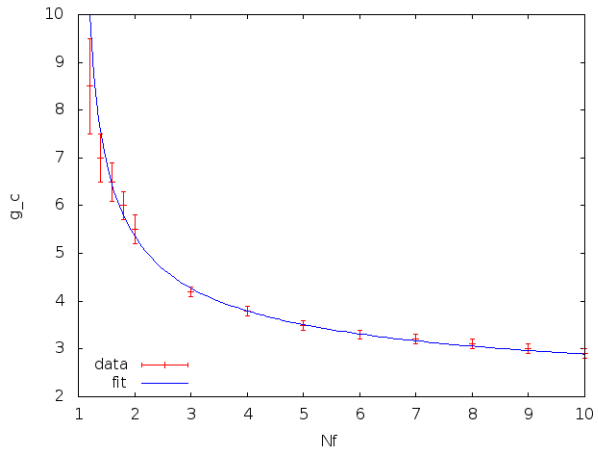

Figure 4.2: Combination of our $N_f \in (1, 2]$ and Javernick's $N_f > 2$ coupling data along with their optimized fit $g_c^{\text{fit}}(N_f) = 1.66 + 3.70(N_f - 1)^{-0.50}$. The fit appears to be qualitatively accurate, and the relatively low root-mean-square error $E_{rms} = 1.05$ further suggests that our predicted model Eq. (2.27) is a viable candidate for the true analytic form for $g_c(N_f)$.

Chapter 5

Summary and Conclusions

We have shown that our computer program – designed to calculate the ground-state energies of systems of distinguishable particles that interact via an attractive two-body contact potential – produces the expected qualitative relationship between the bare coupling and the ground-state energy, namely the existence of a critical coupling above which the energy becomes negative. We have also shown that this critical coupling g_c depends on the number of particle flavors N_f that make up the system; in particular, that $g_c(N_f)$ begins to diverge to infinity as N_f decreases towards unity. Furthermore, by calculating the critical coupling for $N_f \in (1, 2]$ and combining our data with Javernick's $N_f > 2$ data, we were able to apply a fit to our predicted model for $g_c(N_f)$ and obtain the approximate analytic form $g_c(N_f) \approx g_c^{\text{fit}}(N_f) = 1.66 + 3.70(N_f - 1)^{-0.50}$. This fit agrees with our data to relatively high accuracy ($E_{rms} = 1.05$), suggesting that our predicted model is indeed a viable candidate for the true analytic form for $g_c(N_f)$.

If our model is indeed correct and our optimized parameters $(a, b, c) = (1.66, 3.70, 0.50)$ are in the vicinity of the true parameter values, the implications would be interesting. If the true value of c is exactly $1/2$ (as opposed to some arbitrary constant near 0.50), it could indicate that there is an underlying physical or mathematical explanation for the exact analytic form of $g_c(N_f)$. Even more interesting are the implications of having $a > 0$. Since $g_c(N_f) \to a$ as $N_f \to \infty$, having $a > 0$ would mean that no matter how many distinguishable particles there are in a system governed by an attractive two-body contact potential, there is always a non-trivial minimum coupling needed for bound-state formation to occur. This phenomenon would be somewhat counter-intuitive; since the potential energy of the system (see Section 2.1) appears to go like $V \sim -gN_f$, one might expect that putting a large number of particles (e.g., $N_f = 100$) into a system would mean that a very small coupling (e.g., $g \sim 0.01$) would still be large enough to make V sufficiently negative for a bound state to form. Therefore, if it is indeed true that $g_c(\infty) > 0$, there must be something more subtle occurring. In order to increase the precision of the fitting parameters (a, b, c) and determine whether this bizarre phenomenon actually occurs, further research must be conducted.

Acknowledgments

I would like to especially thank my advisor Dr. Joaquín Drut for his endless patience and guidance throughout this project. I would also like to thank Philip Javernick for allowing me to include his data in this paper, as well Andrew Loheac and William J. Porter for their assistance with some of the technical computational and theoretical aspects of the project. This material is based upon work supported by the National Science Foundation under Grants No. PHY1306520 (Nuclear Theory Program) and PHY1452635 (Computational Physics Program).

References

[1] V. N. Efimov, Phys. Lett. B **33**, 563 (1970).

[2] V. N. Efimov, Sov. J. Nucl. Phys. **12**, 589 (1971).

[3] F. Ferlaino, R. Grimm, Physics **3**, 9 (2010).

[4] G. Modugno, Physics **7**, 51 (2014).

[5] P. Courteille, R. S. Freeland, D. J. Heinzen, F. A. van Abeelen, and B. J. Verhaar, Phys. Rev. Lett., **81** (1998) 69.

[6] J. E. Drut and A. N. Nicholson, J. Phys. G **40**, 043101 (2013).

[7] R. L. Stratonovich, Sov. Phys. Dokl. **2** (1958) 416.

[8] J. Hubbard, Phys. Rev. Lett. **3** (1959) 77.

[9] L. Rammelmüller, W. J. Porter, A. C. Loheac, J. E. Drut, arXiv:1505.02131.

[10] L. Rammelmüller, W. J. Porter, J. E. Drut, arXiv:1505.09361.

[11] S. Duane, A. D. Kennedy, B. J. Pendleton, D. Roweth, Phys. Lett. B, **195**, 216 (1987).

[12] R. M. Neal, arXiv:1206.1901.